



CHALMERS



Advanced and Fault-tolerant Control of a BLDC Motor

A Study of Possible Improvements to an Existing Control Method and the Development of an Open-Loop Strategy

Degree Project in the Bachelor's Programme in Mechatronics Engineering

Hannes Torgnysson
Johan Martinsson

DEPARTMENT OF ELECTRICAL ENGINEERING

CHALMERS UNIVERSITY OF TECHNOLOGY

Gothenburg 2026

www.chalmers.se

DEGREE PROJECT 2026

Advanced and Fault-tolerant Control of a BLDC Motor

A Study of Possible Improvements to an Existing Control Method
and the Development of an Open-Loop Strategy

HANNES TORGNYSOON
JOHAN MARTINSSON



CHALMERS

DEPARTMENT OF ELECTRICAL ENGINEERING
CHALMERS UNIVERSITY OF TECHNOLOGY
Gothenburg 2026

Advanced and Fault-tolerant Control of a BLDC Motor
A Study of Possible Improvements to an Existing Control Method and the Development of an Open-Loop Strategy
HANNES TORGNYSOON
JOHAN MARTINSSON

© HANNES TORGNYSOON, 2026.

© JOHAN MARTINSSON, 2026.

Supervisor: Johan Hellsing, InfiMotion Technology Europe AB
Examiner: Bertil Thomas, Department of Electrical Engineering

Degree Project 2026
Department of Electrical Engineering
Chalmers University of Technology
SE-412 96 Göteborg
Phone +46 31 772 1000

Cover: An EDU from InfiMotion.

Written in L^AT_EX
Gothenburg 2026

Acknowledgements

This thesis project was carried out at InfiMotion Technology Europe AB. The project was conducted as part of the Bachelor's Programme in Mechatronics Engineering at the Department of Electrical Engineering. Bertil Thomas served as our supervisor and examiner, and we would like to give him a special thank you for his support throughout the project.

We would like to thank InfiMotion Technology Europe AB for giving us the opportunity to carry out this project at the company. The project has provided us with valuable insights into how the automotive industry operates and what it is like to work in a professional engineering environment. We would also like to express our sincere gratitude to Johan Hellsing and Tobias Berndtson, who were the two people at InfiMotion that we worked most closely with throughout the project. We will never forget the many valuable discussions we had during the weekly meetings throughout the project.

We would also like to thank Henrik Brenander, Per Hillerborg, and Kaixin Chen for all the support and assistance they provided during the final stage of the project, when everything was implemented and tested.

Hannes Torgnysson and Johan Martinsson, Gothenburg, May 2026

Advanced and Fault-tolerant Control of a BLDC Motor
A Study of Possible Improvements to an Existing Control Method and the Development of an Open-Loop Strategy
HANNES TORGNYSOON
JOHAN MARTINSSON
Department of Electrical Engineering
Chalmers University of Technology

Abstract

This thesis examines the control of a brushless direct current (BLDC) motor used to actuate the park lock and the disengagement clutch in an electric drive unit (EDU) for automotive applications. The primary objective is to enhance the performance of an existing control strategy while developing a complementary open-loop fault-detection method. The motivation for this work stems from opportunities to further improve the existing implementation, where timing inaccuracies during commutation can affect acoustic noise levels and motor smoothness. To address this, the first objective was to improve the existing trapezoidal commutation method by increasing the interrupt frequency from 10 kHz to 15 kHz, thereby enhancing the control system's temporal resolution. This modification enables more frequent updates to rotor position, commutation states, and pulse-width modulation (PWM) signals, thereby improving control accuracy.

Experimental results show that the enhanced method maintains comparable performance at lower speeds while providing smoother operation and reduced noise at higher speeds. The second objective was to develop a sensorless open-loop control strategy that operates the motor without Hall-effect sensor feedback, enabling fault detection when the closed-loop system becomes inoperative due to sensor failure. In this approach, the rotor is first aligned to known positions and then driven through a full mechanical rotation using predefined commutation timing. Overall, the results demonstrate that relatively simple modifications can significantly improve control performance, while the proposed open-loop method offers potential for increased system robustness, although further work is required for practical implementation and validation.

Keywords: BLDC motor, Electric Drive Unit (EDU), Trapezoidal commutation, Interrupt frequency, Pulse-width modulation (PWM), Motor control optimization, Acoustic noise reduction, Open-loop control, Sensorless operation, Fault detection.

Contents

1	Introduction	1
1.1	Background	1
1.2	Aim	1
1.3	Objectives	2
1.4	Limitations	2
2	Theory	3
2.1	BLDC Motor with Hall-effect Sensors	3
2.2	Commutation Strategies	4
2.2.1	Trapezoidal Commutation	4
2.2.2	Sinusoidal Commutation	6
2.2.3	Field Oriented Control	6
2.2.4	Open-Loop	10
3	Methodology	11
4	Implementation	13
4.1	Previous Solution	13
4.2	New Solution	15
4.3	Proposed Open-Loop Solution	16
4.4	Test Procedure	16
5	Results	19
5.1	Results for Objective 1	19
5.2	Results for Objective 2	21
6	Conclusion & Discussion	23
6.1	Discussion of the Results	23
6.2	Future Work and Alternative Solutions	23
6.3	Sustainability	25
	Bibliography	27
A	Pictures of the BLDC motor	I

Abbreviations

Below is the list of acronyms that have been used throughout this thesis listed in alphabetical order:

BLDC	Brushless Direct Current
DC	Direct Current
EDU	Electric Drive Unit
EMF	Electromotive Force
FOC	Field-Oriented Control
HIL	Hardware-in-the-Loop
NVH	Noise, vibration, and harshness
PI	Proportional-Integral
PID	Proportional-Integral-Derivative
PMSM	Permanent Magnet Synchronous Motor
PWM	Pulse Width Modulation
RPM	Revolutions Per Minute

Nomenclature

Below is the nomenclature of variables that have been used throughout this thesis.

Variables

T	Motor torque
T_{max}	Maximum motor torque
T_{min}	Minimum motor torque
I_d	Direct-axis current component
I_q	Quadrature-axis current component
I_U	Phase U current
I_V	Phase V current
I_W	Phase W current
I_α	Alpha-axis current component
I_β	Beta-axis current component
α	Alpha-axis stationary reference component
β	Beta-axis stationary reference component
θ_e	Electrical angle
δ	Angle between rotor and stator field
ω_m	Mechanical angular velocity
ω_e	Electrical angular velocity
t	Time

1

Introduction

Modern road vehicles are required to incorporate a robust and reliable parking brake system to ensure that the vehicle cannot move when stationary. The park lock is one of the mechanisms that prevents unintended motion of the vehicle. In practice, the park lock mechanically locks the gearbox, preventing the wheels from rotating.

InfiMotion develops, manufactures, and sells electric drive units (EDUs). To actuate the park lock in their EDU, a brushless direct current (BLDC) motor has been chosen. The same type of motor can also be used to actuate the EDU's disengagement clutch in the vehicle. This functionality allows selective engagement or disengagement of the EDU, depending on operating requirements. This can, for example, reduce energy consumption and increase the driving range.

1.1 Background

InfiMotion currently has a robust implementation, with identified opportunities to further enhance motor performance, particularly regarding torque smoothness and noise, vibration, and harshness (NVH).

In the existing BLDC motor, the rotor's position is estimated using three Hall-effect sensors integrated into the motor. The motor's rotational motion is transmitted through a ball screw mechanism, which converts rotation into linear displacement of a translating nut. This axial movement enables the engagement or disengagement of the park lock or the disconnect clutch.

1.2 Aim

The aim of this project is divided into two objectives. The first objective is to develop an improved control method for the BLDC motor compared to the one currently used at InfiMotion. This means that the new control method should run the motor more smoothly and with less noise while still meeting the performance requirements.

The second objective is to design an open-loop control method, i.e., a method that does not rely on the three Hall-effect sensors. This method is needed to detect a faulty Hall-effect sensor. InfiMotion has an existing fault detection method, but it requires the motor to rotate. However, if one sensor is faulty, the motor cannot

be driven using the existing closed-loop control. Therefore, an open-loop control method is necessary to identify the faulty sensor.

1.3 Objectives

- Objective 1: Can an improved control method run the motor more smoothly and with less noise while still meeting the performance requirements?
- Objective 2: Is it possible to operate the BLDC motor if one or more of the three Hall-effect sensors are faulty with an open-loop control method?

1.4 Limitations

This project has several limitations. One limitation is that the project focuses only on the current motor used by InfiMotion, and it is not possible to change to another motor. The results of the project will only be tested in a laboratory environment and not in a real vehicle.

If it is possible to operate the motor with a faulty sensor, another limitation is that lower performance requirements are acceptable in this case. A final limitation is the project duration, as the project must be completed before June 2026.

2

Theory

This chapter presents the theoretical background required to understand the operation and control of BLDC motors. It introduces the fundamental structure and working principles of BLDC motors, followed by an overview of different commutation strategies, including trapezoidal, sinusoidal, and field-oriented control. Finally, the concept of open-loop control is discussed in the context of motor operation without feedback. Together, these topics provide the foundation for the control methods and improvements investigated in this thesis.

2.1 BLDC Motor with Hall-effect Sensors

A BLDC motor consists of a rotor and a stator. The rotor is equipped with permanent magnets, while the stator contains electromagnetic coils. These coils are divided into three phases. Instead of relying on brushes, as in a conventional DC motor, the motor is controlled by an electronic control unit. Since no brushes are in contact with the rotor, this type of motor typically operates more quietly, generates less heat, and has a longer lifespan compared to a conventional DC motor [1].

The operating principle of a BLDC motor is based on generating a rotating magnetic field by energizing the coils in a specific sequence between the three phases. To determine when to switch to the next phase, three Hall-effect sensors are used to detect the rotor position. The interaction between the stator's rotating magnetic field and the rotor's permanent magnets generates a torque, which causes the rotor to continuously align with the stator field and thereby produce rotational motion [1].

The BLDC motor used by InfiMotion has 7 pole pairs in the rotor and 12 electromagnetic coils in the stator. See Appendix A for pictures of the BLDC motor. The 7 pole pairs are grouped into three phases, as shown in Figure 2.1.

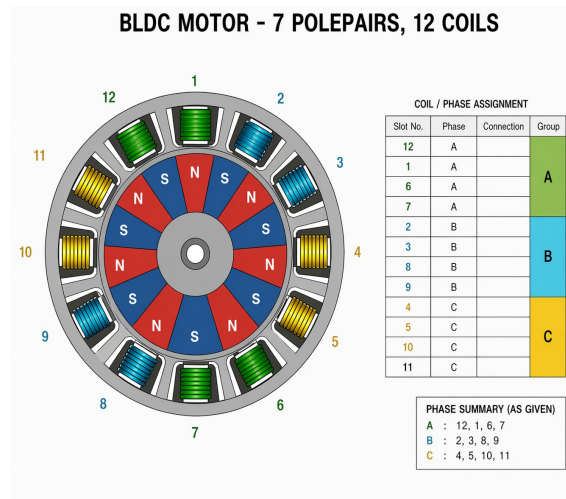


Figure 2.1: InfiMotion’s BLDC motor layout. (Created with ChatGPT, 2026)

2.2 Commutation Strategies

This section presents the most common commutation strategies for controlling a BLDC motor.

2.2.1 Trapezoidal Commutation

Trapezoidal commutation is one of the simplest methods for controlling a BLDC motor. Using information from the three Hall-effect sensors, a resolution of 60 degrees is obtained for the rotor position. This information is then used to activate the correct phase at the right time. It can be seen as the rotor position being divided into six sectors, and depending on which sector the rotor is in, the phases are connected to either +, -, or floating (0) [2]. See Table 2.1 below.

Table 2.1: Commutation sequence for BLDC motor [2].

Interval in degrees	Sector	Phase A	Phase B	Phase C
0 - 60	0	+	-	0
60 - 120	1	+	0	-
120 - 180	2	0	+	-
180 - 240	3	-	+	0
240 - 300	4	-	0	+
300 - 360	5	0	-	+

By doing this, the phases are energized so that the angle between the stator and rotor fields produces maximum torque. This leads to a rotating magnetic field. This field rotates with the so-called electrical frequency. This rotating field then causes the rotor to rotate with the frequency $\frac{\text{Electrical frequency}}{\text{Number of pole pairs}}$ [2].

The magnitude of the torque that causes the rotor to rotate is at its maximum when the angle between the stator field and the rotor field is 90 degrees. Since the stator field changes in discrete 60-degree steps while the rotor field rotates continuously, the torque will vary. The angle between the stator field and the rotor field is 90 degrees in the middle of a sector, which means that the angle between the fields will be 60 degrees at the beginning and 120 degrees at the end of each sector. This therefore results in a lower torque at the beginning and end of each sector. This is shown in (2.1) below [2].

$$T_{\min} = T_{\max} \cdot \sin(60^\circ) = T_{\max} \cdot \sin(120^\circ) = T_{\max} \cdot 0.87 \quad (2.1)$$

This shows that the torque will vary by approximately 13%.

The average torque over one sector can be calculated by integrating the torque between 60° and 120°. Since integration is performed in radians, these angles correspond to

$$60^\circ = \frac{\pi}{3}, \quad 120^\circ = \frac{2\pi}{3}. \quad (2.2)$$

The interval length therefore becomes

$$\frac{2\pi}{3} - \frac{\pi}{3} = \frac{\pi}{3}. \quad (2.3)$$

The average value of a function over an interval is obtained by dividing the integral by the interval length. Thus, the average torque becomes

$$T_{avg} = \frac{1}{\pi/3} \int_{\pi/3}^{2\pi/3} T_{max} \sin(\theta_e) d\theta_e \quad (2.4)$$

$$T_{avg} = \frac{T_{max}}{\pi/3} [-\cos(\theta_e)]_{\pi/3}^{2\pi/3} \quad (2.5)$$

$$T_{avg} = \frac{T_{max}}{\pi/3} \left(-\cos\left(\frac{2\pi}{3}\right) + \cos\left(\frac{\pi}{3}\right) \right) \quad (2.6)$$

$$T_{avg} = \frac{T_{max}}{\pi/3} (0.5 + 0.5) \quad (2.7)$$

$$T_{avg} = \frac{3}{\pi} T_{max} \approx 0.955 T_{max}. \quad (2.8)$$

The advantages of trapezoidal commutation are that the method is simple to understand and implement. The disadvantages, however, are that at low speeds the motor may move in a jerky manner and generate noise. This is partly due to the fact that at low speeds, the phases also switch less frequently, which makes the variations in torque even more noticeable [2].

2.2.2 Sinusoidal Commutation

Instead of trapezoidal control, sinusoidal commutation can be used. This means that the three phases are energized with sinusoidal currents. In sinusoidal commutation, all three phases are always active, compared to trapezoidal commutation where one phase is always floating [3].

These sinusoidal waveforms must match the rotor position, and therefore, a resolution of 60 degrees is not sufficient. Typically, a resolution of 1 degree or less is required. The higher the resolution, the better the commutation performance. Therefore, it is optimal to use a continuous position sensor. It is also possible to use an interpolation method based on three Hall-effect sensors, but this does not provide the same accuracy as a continuous position sensor and is more complex to implement [3].

The advantage of this method is that it provides smooth torque even at low speeds due to better flux alignment. However, the disadvantage is that at higher speeds, a lower torque is obtained compared to trapezoidal control. This is because the back-EMF increases with speed, thereby reducing the voltage available to drive the motor. Since the phase voltages are sinusoidal, they only reach their maximum value for a short duration, in contrast to trapezoidal control where the voltage remains close to its maximum for a longer time. This means that the effective voltage driving the motor is lower in sinusoidal commutation, which results in lower torque at higher speeds [3].

2.2.3 Field Oriented Control

Field-Oriented Control (FOC) is an advanced control method that enables precise and dynamic regulation of torque and flux in brushless DC (BLDC) and permanent-magnet synchronous motors (PMSMs). The technique relies on mathematically transforming the three-phase motor currents into a rotating reference frame aligned with the rotor's magnetic field. This transformation allows the control problem to be treated as two independent current components, enabling optimization of torque production, dynamic response, and overall efficiency [2].

To generate torque in an electric motor, the stator magnetic field vector must lead the rotor field vector by a specific angle. The torque increases as the angle between these vectors increases, and maximum torque is achieved when the stator field vector is orthogonal to the rotor field vector. In FOC, this condition is achieved by first determining the rotor position, then commanding a stator field vector offset by 90 degrees relative to the rotor field. By precisely regulating the three-phase currents, the controller can generate the desired stator field vector, as illustrated conceptually in Figure 2.2 [4].

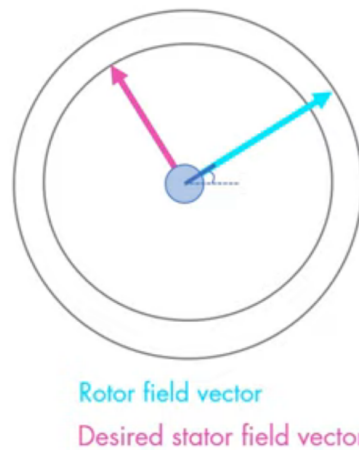


Figure 2.2: Rotor and stator field vectors. [4]. Public Domain

To compute this desired stator field vector, it is decomposed into two orthogonal components in the rotating reference frame, as illustrated in Figure 2.3. These are the direct axis component (d -axis), which is aligned with the rotor magnetic field, and the quadrature axis component (q -axis), which is orthogonal to it. In torque-controlled applications, the FOC algorithm drives the direct component I_d toward zero to minimize unwanted field-weakening effects, while the quadrature component I_q is regulated to generate the commanded torque [4].

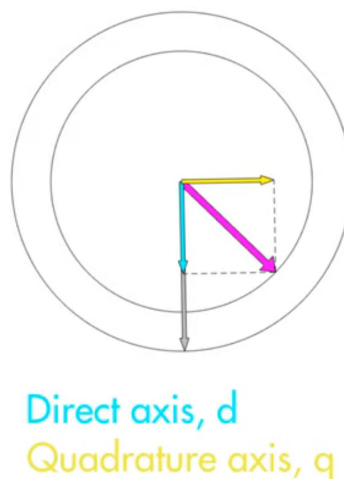


Figure 2.3: Stator field vector components. [4]. Public Domain

The mathematical conversion from the three-phase currents (I_U, I_V, I_W) to the rotating reference frame currents (I_d, I_q) is performed in two steps. First, the Clarke transformation maps the three-phase currents to the stationary two-axis (α, β) reference frame, as defined in Equations (2.9). Although this reduces the system from three variables to two, the resulting currents I_α and I_β are still expressed in the stator-fixed coordinate system Figure 2.4. To rotate these currents into the

rotor-aligned reference frame Figure 2.5, the Park transformation is applied, resulting in the (I_d, I_q) components as shown in Equations (2.10) [4].

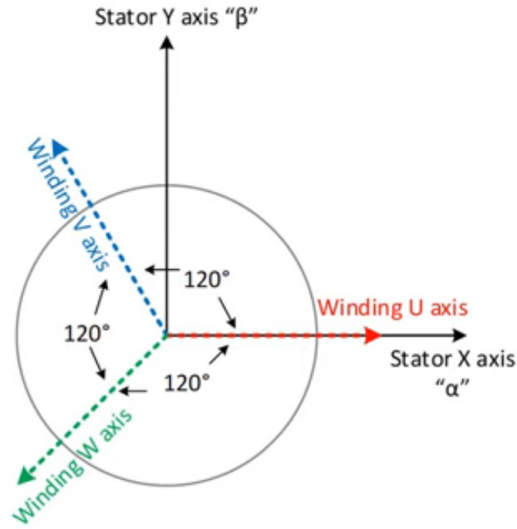


Figure 2.4: Stator-based coordinate system. [4]. Public Domain

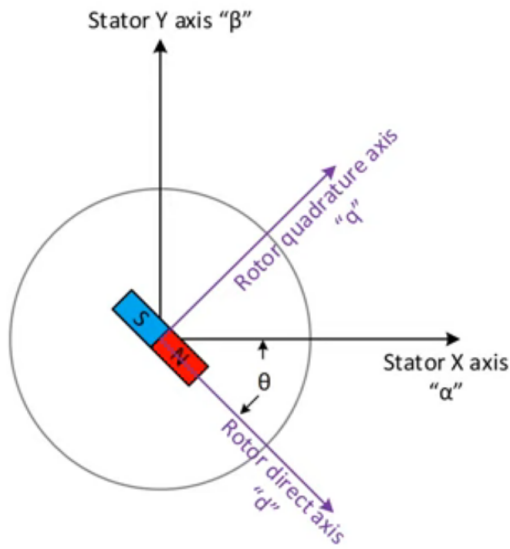


Figure 2.5: Rotor-based coordinate system. [4]. Public Domain

$$I_U, I_V, I_W \rightarrow I_\alpha, I_\beta \tag{2.9a}$$

$$\alpha = U_\alpha + V_\alpha + W_\alpha \quad (2.9b)$$

$$\alpha = U + V \cos(120^\circ) + W \cos(240^\circ) \quad (2.9c)$$

$$\alpha = U - \frac{1}{2}V - \frac{1}{2}W \quad (2.9d)$$

$$\beta = U_\beta + V_\beta + W_\beta \quad (2.9e)$$

$$\beta = U + V \sin(120^\circ) + W \sin(240^\circ) \quad (2.9f)$$

$$\beta = \frac{\sqrt{3}}{2}V - \frac{\sqrt{3}}{2}W \quad (2.9g)$$

$$I_\alpha, I_\beta \rightarrow I_d, I_q, \quad (2.10a)$$

$$d = \alpha_d + \beta_d \quad (2.10b)$$

$$d = \alpha \cos(\theta_e) + \beta \sin(\theta_e) \quad (2.10c)$$

$$q = \alpha_q + \beta_q \quad (2.10d)$$

$$q = \alpha \sin(\theta_e) + \beta \cos(\theta_e) \quad (2.10e)$$

These two current components are independently controlled using proportional-integral (PI) or proportional-integral-derivative (PID) controllers, which allow the system to track the desired torque and flux-producing currents. The controller outputs are then transformed back to three-phase voltages using the inverse Park and Clarke transformations. These voltages are supplied to the inverter, which applies the corresponding switching states to the motor. The resulting currents and estimated rotor position form a closed-loop system in which the motor speed and torque follow the commanded inputs with high accuracy, as illustrated by Figure 2.6 [5].

Field-oriented control provides smooth, instantaneous, and ripple-free torque generation across the entire speed range, while also minimizing acoustic and electrical noise. However, this performance comes at the cost of increased computational complexity, requiring accurate position feedback, rapid current sampling, and real-time execution of several coordinate transformations and control loops.

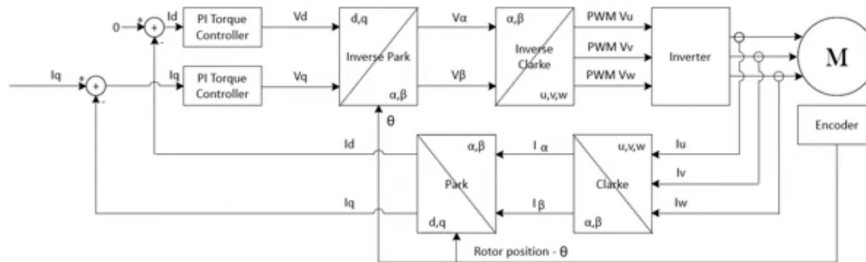


Figure 2.6: Control block diagram - FOC. [5]. Public Domain

2.2.4 Open-Loop

An open-loop control strategy for an electric motor and specifically for a BLDC motor, refers to a control method in which the commutation sequence and switching signals are generated without feedback from the motor's actual position, speed, or torque. Instead, the controller operates solely on predefined control parameters and timing assumptions, effectively assuming ideal and predictable system behavior.

In an open-loop BLDC drive, a fixed or predetermined duty cycle is typically applied to the inverter. Based on the expected motor characteristics such as rated speed, load conditions, and electrical time constants, the controller estimates the time required for the rotor to advance from one commutation sector to the next. The commutation instants are therefore scheduled according to these calculated time intervals rather than being triggered by position sensors or by estimated rotor position [6].

This approach significantly simplifies the control system by eliminating the need for sensors, observer algorithms, or feedback loops. However, the lack of feedback makes open-loop control sensitive to parameter variations and external disturbances. Changes in load torque, supply voltage, temperature, or motor parameters can lead to deviations between the assumed and actual rotor position. As a result, incorrect commutation timing may occur, potentially reducing efficiency, increasing torque ripple, or even causing loss of synchronization at higher loads or low speeds. Due to these limitations, open-loop control of BLDC motors is primarily suitable for applications with relatively constant and predictable operating conditions, such as low-cost systems, fans, or pumps, and for specific operating phases, such as initial startup before closed-loop control is engaged.

3

Methodology

This project will be carried out in a step-by-step manner to ensure a result that meets the defined requirements. The same methodology is used to achieve both objectives.

1. **Feasibility study and literature review:** The project starts with a feasibility study to gain a better understanding of the scope, objectives, and potential challenges. This is later followed by a literature study about electric machines, with a specific focus on BLDC motors and control methods.
2. **Control method development:** Based on the results of the literature study, a set of different control methods is evaluated and compared. Factors such as speed, response time, efficiency, and overall performance are considered. The most promising method is then selected.
3. **Implementation and evaluation:** The chosen control method is implemented in the selected environment, either in a simulation or on a physical BLDC motor. Its performance is then evaluated against the defined requirements, with a focus on speed, noise, and smoothness. If the method does not fully meet the requirements, adjustments are made to improve performance. This iterative process continues until the results are acceptable.
4. **Communication:** During the course of the project, weekly meetings will be held involving the company supervisor, the thesis workers, and relevant company specialists. These meetings serve as a structured forum for monitoring project progress, addressing technical challenges, and ensuring alignment between all stakeholders. Regular interaction helps to identify potential issues at an early stage, thereby reducing the risk of delays, misunderstandings, or miscommunication. In addition to the scheduled meetings, communication will continue via Microsoft Teams and email. A dedicated Teams group will be established to facilitate efficient information sharing, document exchange, and ongoing discussions. This digital communication channel ensures accessibility and transparency, allowing all participants to stay updated on project developments and contribute when necessary.

4

Implementation

This chapter presents the implementation of the control methods investigated in this project, including both the previous solution and the proposed improvements.

4.1 Previous Solution

The original control method implemented for the BLDC motor was a variant of trapezoidal commutation, commonly referred to as “pulling.” In this implementation, commutation was achieved using a discrete-time approach based on a hardware timer. The timer was configured to generate periodic interrupts at fixed intervals, triggering the execution of the motor control routine. The timer was set to $100 \mu s$. During each interrupt, the rotor position was determined through Hall-effect sensor feedback. Based on the identified rotor sector, the corresponding commutation step was applied by switching the phase voltages in accordance with a predefined sequence.

The time-driven nature of the control algorithm implies that commutation was not continuously synchronized with the exact rotor position but was instead approximated at discrete time instances. Although this approach is sufficient for operation at low to moderate speeds, it may introduce torque variations at high speeds.

The equations below show that at 4000 rpm , the motor rotates approximately 16.8° electrical degrees during $100 \mu s$. This means that, in the worst-case scenario, the rotor may rotate 16.8° into the next sector before the commutation is updated to the correct phase.

The corresponding mechanical angular velocity is

$$\omega_m = \frac{4000 \cdot 2\pi}{60} = 418.88 \text{ rad/s.} \quad (4.1)$$

This gives the electrical angular velocity

$$\omega_e = 7 \cdot 418.88 = 2932.15 \text{ rad/s.} \quad (4.2)$$

The electrical angle rotated during $100 \mu s$ is calculated as

$$\theta_e = \omega_e \cdot t \quad (4.3)$$

4. Implementation

where

$$t = 100 \times 10^{-6} s. \quad (4.4)$$

Thus,

$$\theta_e = 2932.15 \cdot 100 \times 10^{-6} = 0.2932 \text{ rad}. \quad (4.5)$$

Converted to degrees,

$$\theta_e = 0.2932 \cdot \frac{180}{\pi} \approx 16.8^\circ. \quad (4.6)$$

Therefore, the motor rotates approximately 16.8 degrees during 100 μs .

This introduces a problem because the torque becomes discontinuous. When the rotor continues too far into the next sector before commutation occurs, the angle between the rotor and stator magnetic fields deviates from its optimal value. As a result, the produced torque decreases. When the commutation finally switches to the correct sector, the torque suddenly increases again. This results in torque ripple rather than a smooth, continuous torque output.

Figure 4.1 below shows how the delayed commutation leads to a discontinuous torque.

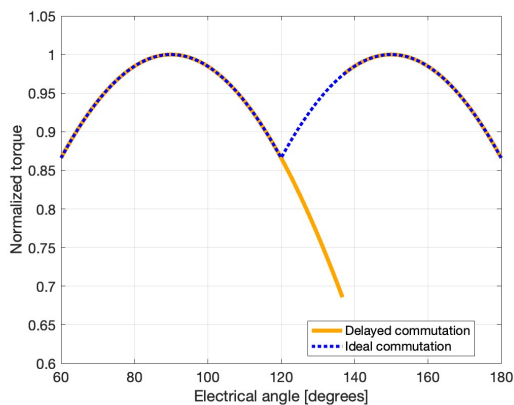


Figure 4.1: Illustration of torque ripple caused by delayed commutation.

However, the method offers low computational complexity and is easy to implement, making it suitable for systems with limited processing capabilities.

Simultaneously, the pulse-width modulation (PWM) duty cycle was updated in the same interrupt routine. The PWM signal determines the average voltage applied to the motor phases, thereby controlling the motor's torque and speed. By adjusting the duty cycle, the motor's operating point was regulated. Integration of position evaluation, commutation, and duty-cycle update within a single interrupt simplifies the control structure, albeit at the cost of reduced temporal resolution. A key limitation of this approach is that commutation occurs at fixed time intervals rather

than precisely aligning with the motor's electromagnetic state. This can result in torque ripple, current distortion, and increased acoustic noise and mechanical vibration. Despite these drawbacks, the method remains suitable for applications with moderate performance requirements.

4.2 New Solution

The improved control strategy implemented in this work is based on the same trapezoidal commutation framework as the original method. The primary modification concerns the configuration of the interrupt timer that governs the execution rate of the control routine. In the original implementation, the timer operated at a frequency of 10 kHz , corresponding to an interrupt period of $100\ \mu\text{s}$. Given the application context, in which the BLDC motor actuates a parking brake mechanism, the system experiences rapid acceleration and deceleration over short time intervals. Under such operating conditions, the relatively long interrupt period may limit the temporal resolution of the control system. In particular, rotor position updates, commutation events, and duty cycle adjustments are only performed at discrete time instances defined by the interrupt frequency. This can introduce a mismatch between the actual rotor position and the applied commutation state during fast transients.

To address this limitation, the interrupt frequency was increased from 10 kHz to 15 kHz , resulting in a reduced sampling period of approximately $67\ \mu\text{s}$. This implies that, in the new worst-case scenario, the rotor may rotate 11.2° into the next sector before the commutation is updated to the correct phase.

The corresponding mechanical angular velocity is

$$\omega_m = \frac{4000 \cdot 2\pi}{60} = 418.88\text{ rad/s}. \quad (4.7)$$

This gives the electrical angular velocity

$$\omega_e = 7 \cdot 418.88 = 2932.15\text{ rad/s}. \quad (4.8)$$

The electrical angle rotated during $67\ \mu\text{s}$ is calculated as

$$\theta_e = \omega_e \cdot t \quad (4.9)$$

where

$$t = 67 \times 10^{-6}\text{ s}. \quad (4.10)$$

Thus,

$$\theta_e = 2932.15 \cdot 67 \times 10^{-6} = 0.1964\text{ rad}. \quad (4.11)$$

Converted to degrees,

$$\theta_e = 0.1964 \cdot \frac{180}{\pi} \approx 11.2^\circ. \quad (4.12)$$

Therefore, the motor rotates approximately 11.2 degrees during 67 μs .

This modification increases the execution rate of the control routine, allowing more frequent updates to rotor position estimation, commutation state, and PWM duty cycle. The intended effect of this change is to reduce the maximum timing error between the actual rotor position and the applied commutation state. By improving the temporal resolution of the control loop, the commutation events are expected to more closely follow the motor's electromagnetic behavior, particularly during rapid speed variations. Consequently, this adjustment is anticipated to improve operational smoothness by reducing torque ripple and minimizing acoustic noise.

It should be noted that the increase in interrupt frequency results in a higher computational load, as the control routine must be executed more frequently. However, due to the relatively low complexity of the trapezoidal commutation algorithm, this modification is considered feasible within the constraints of the target hardware platform. In summary, the implemented improvement retains the original control structure while modifying the system's timing characteristics. The increase in interrupt frequency is intended to enhance control accuracy during dynamic operation by providing finer temporal resolution without introducing additional algorithmic complexity.

4.3 Proposed Open-Loop Solution

The secondary part of the project was to develop a sensorless open-loop control method for the motor. Prototype code was created but never tested due to limited time and resources.

4.4 Test Procedure

To compare the new solution with the previous one, a test was conducted using a Hardware-in-the-Loop (HIL) test rig. The purpose of the test was to evaluate whether the new solution produced different results when a specific PWM value was applied and the resulting motor speed was measured. During the testing, all participants also listened for any differences in noise between the two solutions. To ensure a repeatable and consistent load on the motor, a propeller was mounted on the motor shaft to act as a braking load. See Figure 4.2 below.



Figure 4.2: Test rig.

The test procedure began by operating the motor with the previous solution at different PWM values. The PWM was increased in steps of 10%, starting at 10% and continuing up to 100%. At each PWM level, the motor speed was measured and documented. After all measurements were completed with the previous solution, the exact same procedure was repeated with the new solution to enable a fair comparison between the two control methods.

5

Results

This chapter presents the results for Objective 1 and Objective 2.

5.1 Results for Objective 1

The new solution resulted in minimized torque ripple in the worst-case scenario, which in turn produced a smoother torque curve, as shown in Figure 5.1.

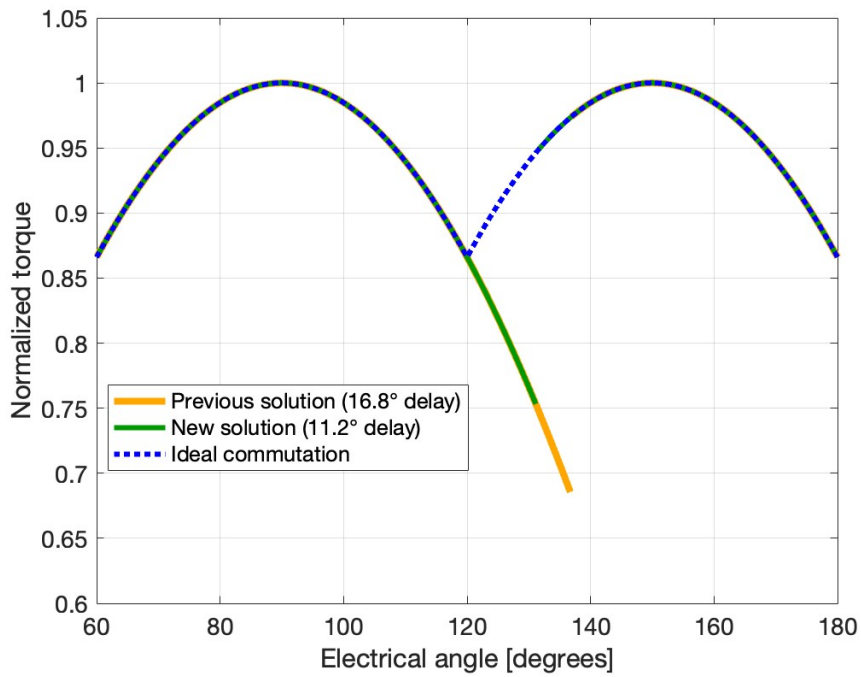


Figure 5.1: Illustration of torque ripple caused by delayed commutation with the new solution.

The average torque over the interval 60° to 180° is calculated over two sectors. The total interval length is

$$180^\circ - 60^\circ = \frac{2\pi}{3}. \quad (5.1)$$

For the previous solution, the commutation delay is 16.8° , which corresponds to

$$\delta_{old} = 16.8^\circ \cdot \frac{\pi}{180} \approx 0.293 \text{ rad.} \quad (5.2)$$

The average torque then becomes

$$T_{avg,old} = \frac{T_{max}}{2\pi/3} \left(\int_{\pi/3}^{2\pi/3} \sin(\theta_e) d\theta_e + \int_{2\pi/3}^{2\pi/3+\delta_{old}} \sin(\theta_e) d\theta_e + \int_{\pi/3+\delta_{old}}^{2\pi/3} \sin(\theta_e) d\theta_e \right) \quad (5.3)$$

$$T_{avg,old} = \frac{T_{max}}{2\pi/3} \left(1 - \cos\left(\frac{2\pi}{3} + \delta_{old}\right) + \cos\left(\frac{\pi}{3} + \delta_{old}\right) \right) \quad (5.4)$$

$$T_{avg,old} \approx 0.935T_{max}. \quad (5.5)$$

For the new solution, the commutation delay is 11.2° , which corresponds to

$$\delta_{new} = 11.2^\circ \cdot \frac{\pi}{180} \approx 0.195 \text{ rad.} \quad (5.6)$$

The average torque then becomes

$$T_{avg,new} = \frac{T_{max}}{2\pi/3} \left(\int_{\pi/3}^{2\pi/3} \sin(\theta_e) d\theta_e + \int_{2\pi/3}^{2\pi/3+\delta_{new}} \sin(\theta_e) d\theta_e + \int_{\pi/3+\delta_{new}}^{2\pi/3} \sin(\theta_e) d\theta_e \right) \quad (5.7)$$

$$T_{avg,new} = \frac{T_{max}}{2\pi/3} \left(1 - \cos\left(\frac{2\pi}{3} + \delta_{new}\right) + \cos\left(\frac{\pi}{3} + \delta_{new}\right) \right) \quad (5.8)$$

$$T_{avg,new} \approx 0.946T_{max}. \quad (5.9)$$

This shows that the average torque increased by approximately 1% with the new solution compared to the previous solution.

The result from the test where the previous solution is compared to the new one is shown in Figure 5.2 below.

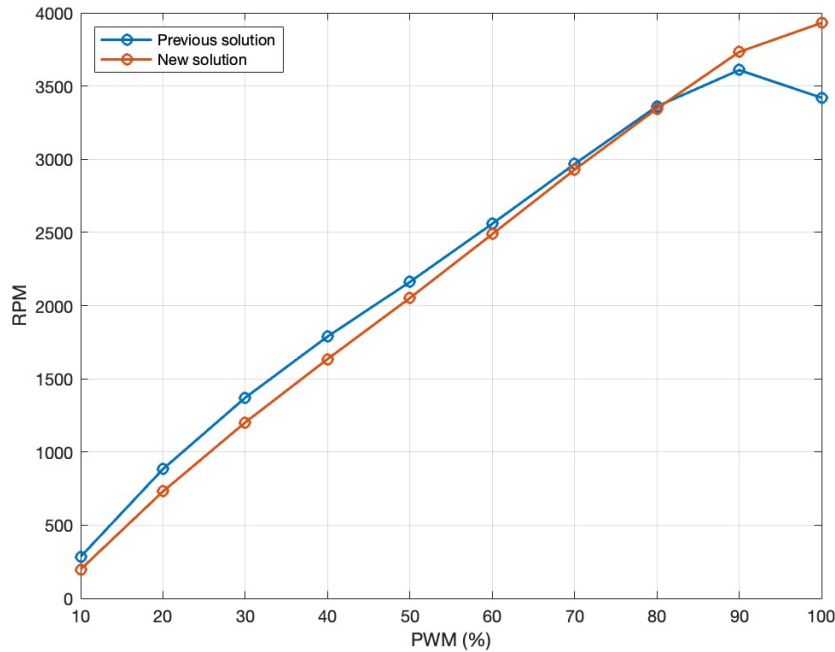


Figure 5.2: Test results.

This shows that the speed is nearly the same for both solutions at low PWM values, whereas the new solution performs better at high PWM values.

During the testing, it was observed by the test participants that the previous solution produced a noticeable high-pitched noise at higher speeds. This noise was no longer present with the new solution. Although this observation was subjective and was not measured or quantified in any way, it is still considered worth mentioning.

5.2 Results for Objective 2

The second objective led to a theoretical implementation describing the operation of the open-loop control strategy. The purpose of the open-loop is to achieve one full mechanical rotation of the rotor without relying on any sensor feedback. As illustrated in Figure 5.3, the process begins with a state-alignment phase, in which the rotor is sequentially driven to two predefined positions. This step ensures a known initial position and guarantees that the rotor starts rotating in the intended direction. Following alignment, the system enters a commutation phase, where the switching sequence is progressively accelerated, causing the motor speed to ramp up. During this phase, the rotor is driven through all electrical sectors until one complete mechanical revolution is achieved. Once the full rotation is complete, the process terminates, and the open-loop sequence stops.



Figure 5.3: Proposed open-loop commutation sequence.

6

Conclusion & Discussion

Overall, we are satisfied with the work and the results achieved. The project has given us valuable insights into how work is carried out in international companies and has been a very rewarding experience. These are experiences that we will bring with us to future studies and workplaces.

6.1 Discussion of the Results

We are generally satisfied with the results the project produced. We analyzed the previous control method and reviewed the literature on possible solutions. We then presented different solution proposals to the company and discussed them together. After that, a joint decision was made on which method to implement and test. The implemented method showed performance comparable to the company's previous solution at low PWM values, while delivering better results at high PWM values in terms of both speed and noise reduction. This was very positive and something we are proud of. Even though our solution is not optimal, it still demonstrates significant opportunities to improve the control system by optimizing the company's previous solution. The results may be affected by external factors, including sensor disturbances caused by ambient light in the test environment. The heat generated by the motor could also affect its overall performance.

Regarding the open-loop control strategy, we developed a proposed solution, but it was never tested due to a lack of resources at the company at the time. It is unfortunate that we never got to see this solution in practice, but we are still satisfied with having developed a proposed solution, and hopefully the company will be able to use our work in the future when they have the time and opportunity to implement it.

6.2 Future Work and Alternative Solutions

With more time and resources, there are several possible continuations of this work regarding improved control methods. One possible improvement would have been to increase the update frequency even further than was achieved in this project to achieve more optimal synchronization between the rotor and the stator. The reason this was not implemented in our work was that the processor could not handle the increased computational load. However, with a more powerful processor capable of

handling greater workloads, this could have been a viable alternative.

Another possible approach would have been to use interrupts triggered directly by the Hall-effect sensors rather than a timer interrupt. This would likely have resulted in the optimal control achievable with trapezoidal commutation. The reason this approach was not tested in this project was that it would have required significant additional work and assistance from other employees at the company, as large parts of the software would have needed to be redesigned. One disadvantage of this solution, however, is that the processor load would be harder to predict, as it would vary with motor speed. From that perspective, a timer-triggered interrupt is preferable, since it keeps the processor load predictable at all times.

A third possible approach would have been to implement sinusoidal commutation or FOC. However, this would have required significantly more resources compared to the previously mentioned alternatives, and therefore changing the control method entirely was never considered a realistic option. While such solutions would likely have yielded even better performance, trapezoidal commutation was considered sufficiently effective for the motor's intended application. The primary goal was therefore to optimize the existing control method rather than replace it completely.

Regarding the open-loop control strategy, the next step would be to implement it in the software and evaluate it in practice. It would also be necessary to determine under which conditions the motor should operate using open-loop control in the future. The purpose of this method is to identify which Hall-effect sensor is malfunctioning, and therefore it would most reasonably be used only when the primary trapezoidal control method fails and there is a need to determine which Hall-effect sensor is defective.

Another possible approach would be for the open-loop method to activate automatically whenever the primary control method stops functioning, for example if the park lock cannot be released. This would prevent the vehicle from becoming immobilized due to a faulty Hall-effect sensor. However, in such a case it would likely be important to provide the user with an error message, since this method does not perform nearly as well as the primary control strategy and the fault would therefore need to be addressed as soon as possible.

6.3 Sustainability

From a sustainability perspective, the improved control method may reduce energy losses and mechanical wear by enabling smoother motor operation and lower torque ripple. By minimizing vibrations and acoustic noise, the system may also improve component lifetime and reduce the need for maintenance or replacement of mechanical parts.

The proposed fault-tolerant open-loop strategy also has an ethical and safety-related significance. A more robust motor control system that can handle sensor faults can increase operational reliability and reduce the risk of failure in safety-critical vehicle functions, such as the park lock mechanism. This may contribute to improved vehicle safety and reliability in future applications.

Bibliography

- [1] IC Components Limited, "Borstlös likströmsmotor – hur den fungerar, typer och fördelar," 2017. [Online]. Available: <https://www.ic-components.se/blog/Brushless-DC-Motor-How-it-Works,Types,and-Benefits.jsp> (accessed on: 2026-04-23).
- [2] C. Nilsson, D. Modrack, "Universal Embedded Motor Control," MSc thesis, Department of Computer Science and Engineering, Chalmers University of Technology, Gothenburg, Sweden, 2013. [Online]. Available: <https://hdl.handle.net/20.500.12380/193773>.
- [3] F. B. Cakar, "Optimal BLDC Motor Control for Autonomous Driving of RC Cars," BSc thesis, Faculty of Informatics, Technische Universität Wien, Vienna, Austria, 2017. [Online]. Available: https://www.auto.tuwien.ac.at/bib/pdf_TR/TR0189.pdf.
- [4] MATLAB, "Understanding Field-Oriented Control | Motor Control, Part 4," YouTube, May. 5, 2020. [Video]. Available: https://www.youtube.com/watch?v=YPD1_rcXBIE.
- [5] Texas Instruments, "Field-Oriented Control," YouTube, March. 2, 2022. [Video]. Available: https://www.youtube.com/watch?v=_6-_jvZe7iA.
- [6] Texas Instruments, "Sensorless startup methods," YouTube, July. 20, 2020. [Video]. Available: <https://www.youtube.com/watch?v=IRFBGb8Q9Wc>.

A

Pictures of the BLDC motor

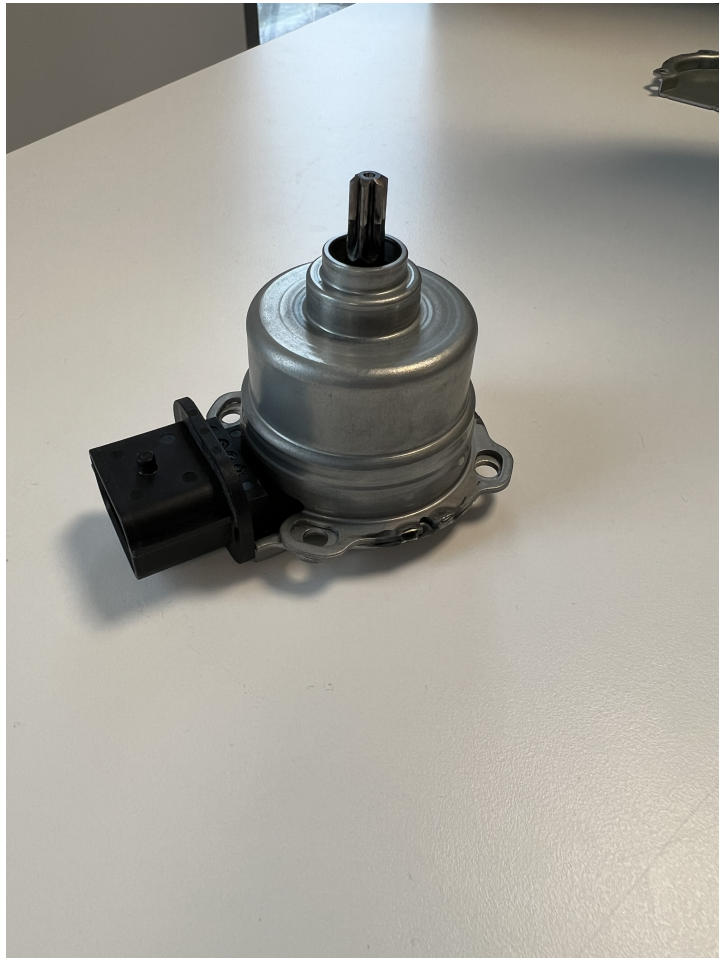


Figure A.1: The BLDC motor.



Figure A.2: The rotor of the BLDC Motor.



Figure A.3: The stator of the BLDC motor.

DEPARTMENT OF ELECTRICAL ENGINEERING
Chalmers University of Technology
Gothenburg, Sweden
www.chalmers.se



CHALMERS